Biochimica et Biophysica Acta 1788 (2009) 1108–1115

Contents lists available at ScienceDirect

Biochimica et Biophysica Acta

journal homepage: www.elsevier.com/locate/bbamem

Structural characterization of the osmosensor ProP

Wajid M.H. Sayeed, John E. Baenziger *

Department of Biochemistry, Microbiology, and Immunology, University of Ottawa, 451 Smyth Rd., Ottawa, Ontario, Canada K1H 8M5

ARTICLE INFO

Article history:
Received 1 October 2008
Received in revised form 9 January 2009
Accepted 21 January 2009
Available online 6 February 2009

Keywords:
Membrane protein
Osmosensing
Fourier-transform infrared spectroscopy
Major facilitator superfamily
ProP
Lac permease

ABSTRACT

ProP, an osmoprotectant symporter from the major facilitator superfamily was expressed, purified and reconstituted into proteoliposomes that are amenable to structural characterization using infrared spectroscopy. Infrared spectra recorded in both ^1H_2O and ^2H_2O buffers reveal amide I band shapes that are characteristic of a predominantly α-helical protein, and that are similar to those recorded from the well-characterized homolog, lactose permease (LacY). Curve-fit analysis shows that ProP and LacY both exhibit a high α-helical content. Both proteins undergo extensive peptide hydrogen–deuterium exchange after exposure to ^2H_2O, but are surprisingly thermally stable with denaturation temperatures greater than 60 °C. 25–30% of the peptide hydrogens in both ProP and LacY are resistant to exchange after 72 h in ^2H_2O at 4 °C. Surprisingly, these exchange resistant peptide hydrogens exchange completely for deuterium at temperatures below those that lead to denaturation. Our results show that ProP adopts a highly α-helical fold similar to that of LacY, and that both transmembrane folds exhibit unusually high temperature-sensitive solvent accessibility. The results provide direct evidence that ProP adopts a structure consistent with other major facilitator superfamily members.

1. Introduction

Membrane transport proteins underlie the cell's ability to maintain homeostasis while adapting to changing environments. The major facilitator superfamily is the largest known family of secondary active transporters, and prototypically consists of a single peptide folded into 12 α-helical transmembrane segments (TM) comprised of two repeated primordial 6-TM peptide motifs [1]. The major facilitator superfamily transporters are found in nearly all organisms, both eukaryotic and prokaryotic. They perform diverse functions ranging from the maintenance of electrochemical gradients to drug resistance [1].

Three members of the major facilitator superfamily have been crystallized, including the lactose permease (LacY) [2,3] from *E. coli*, the oxalate/formate antiporter (OxlT) from *O. formigenes* [4], and the glycerol-3-phosphate transporter (GlpT) from *E. coli* [5]. The detailed structural data now available has given rise to homology models of other major facilitator superfamily transporters, and this has spurred investigation into many transporters that share sequence homology with the aforementioned three proteins. The currently prevailing theory regarding the mechanism of transport centers on an alternating-access model [6]. This model proposes that each protein exists in two conformations that are each "open" to one side of the membrane, and closed to the opposite side. Once substrate binds to the open configuration of the transporter on one side of the bilayer, the transporter then undergoes a conformational change, opening to the opposite side of the bilayer and releasing the substrate. This mechanism necessitates that the core of the protein be exposed to aqueous solvent. The protein must also exhibit large-scale conformational flexibility.

The major facilitator superfamily transporter ProP from *E. coli* is an osmoprotectant symporter that responds to upshifts in external osmolality by transporting H^+ and a broad variety of substrates including ectoine, betaine glycine, and proline into the cell [7], with energy for this process supplied by the proton motive force [8]. A structural model for ProP has been proposed based upon sequence alignments with other major facilitator superfamily members, integrating experimental findings for ProP as well as the structural information provided by the existing crystal structures for LacY and GlpT [9,10]. Direct insight into the structure of ProP and the mechanisms by which it acts as an "osmosensor" are still the subject of speculation and investigation.

Osmosensors have been divided into two categories, which protect the cell from either a hypo-osmolar environment (downshift), or from a hyper-osmolar environment (upshift). The former category is dominated by mechanosensitive channels, which are thought to respond to changes in lateral pressure at the protein–bilayer interface [8]. For the latter category, mechanisms have been tentatively proposed for two proteins besides ProP: the ATP-binding cassette (ABC) transporter, OpuA, and the betaine–carnitine–choline transporter, BetP, neither of which belongs to the major facilitator superfamily. The proposed mechanisms for these two proteins rely on phenomena – such as molecular crowding and changes in ionic strength – that favour or disfavour interactions between a soluble domain of the protein and

* Corresponding author. Tel.: +1 613 562 5800x8222; fax: +1 613 562 5251.
E-mail address: jebaenz@uottawa.ca (J.E. Baenziger).

0005-2736/$ – see front matter © 2009 Elsevier B.V. All rights reserved.
doi:10.1016/j.bbamem.2009.01.010

charged lipid head-groups [8]. In ProP, such a mechanism could potentially involve the C-terminus, which is extended in comparison to ProP paralogues from *E. coli* [9], and which has been shown to mediate in vivo homodimerization of ProP through the formation of an anti-parallel coiled-coil [11]. Although ProP mutants with a C-terminal 26-residue deletion are rendered inactive [12] implicating the C-terminus in osmosensing, recent studies suggest that the coiled-coil modulates, but does not generate the osmoregulatory response [13,14].

As a first step towards understanding the mechanisms of ProP function, we have developed a new procedure for reconstituting ProP into proteoliposomes with lipid–protein ratios that are amenable to structural studies using infrared spectroscopy. Here, we compare the structural and biophysical properties of ProP to those of the well characterized homolog, LacY. Our data show that ProP and LacY both adopt predominantly α-helical secondary structures. Both proteins undergo more extensive peptide hydrogen–deuterium exchange than expected for transmembrane proteins, although 25–30% of the peptide hydrogens are resistant to exchange even after prolonged exposure to ^2H_2O at 4 °C. Relatively high temperatures are required to denature both ProP and LacY. Surprisingly, elevated temperatures below those required to denature both proteins lead to complete peptide hydrogen–deuterium exchange. Our results show that ProP and LacY share a similar transmembrane α-helical fold and exhibit similar biophysical properties including an unusually high temperature-sensitive solvent accessibility.

2. Materials and methods

2.1. Materials

The protease inhibitors leupeptin, aprotinin, soybean trypsin inhibitor, benzamidine and tris(2-carboxyethyl)phosphine were from Calbiochem (La Jolla, CA). Cholate, ampicillin, phenylmethane-sulphonylfluoride, arabinose, lysozyme, β-mercaptoethanol, soybean trypsin inhibitor, and soybean asolectin lipids were from Sigma (Oakville, ON, Canada). DNase was from Roche (Mississauga, ON). Isopropyl β-D-1-thiogalactopyranoside (IPTG) was supplied by MBI Fermentas (Burlington, ON, Canada) and n-Dodecyl β-D-maltoside (DDM) from Anatrace (Maumee, OH). The TALON® Superflow cobalt affinity resin was from Clontech (Mountain View, CA) and the Superdex® gel filtration resin was from GE Healthcare-Biosciences (Piscataway, NJ). *E. coli* polar lipids were purchased from Avanti Polar Lipids (Alabaster, AL). The protein BCA and phospholipids C assay kits were from Pierce Chemicals (Rockford, IL) and Wako Chemicals (Richmond VA), respectively. The phospholipids assay is specific for the choline headgroup.

2.2. Cell growth and protein expression

E. coli strain WG710 was a generous gift of Dr. J.M. Wood (University of Guelph, ON). WG710 corresponds to strain WG350 [F-*trp lacZ rpsL thi* Δ(*putPA*)*101* Δ(*proU*)*600* Δ(*proP-melAB*)212] containing the plasmid pDC80, which was created by inserting the gene encoding ProP-His_6 (C-terminal) behind the arabinose-inducible P_{BAD} promoter of plasmid pBAD24 [12,15,16]. Vector pT7-5/WT-LacY/C$(His)_{10}$ [17] was a generous gift of Dr. H.R. Kaback (UCLA, Los Angeles, CA) and was transformed into *E. coli* C41, a strain that is recommended for the production of membrane proteins [18]. In both cases, single colonies plated on Luria Bertani (LB) Agar, Lennox (5 g/L Tryptone, 5 g/L yeast extract, 5 g/L NaCl, and 15 g/L agar) (BioShop; Burlington, ON, Canada) with 100 μg/mL ampicillin were selected and sub-cultured into 50 mL of LB-Broth, Lennox (5 g/L Tryptone, 5 g/L yeast extract, and 5 g/L NaCl) (BioShop; Burlington, ON, Canada) with 100 μg/mL ampicillin. After overnight growth at 37 °C, the cultures were diluted into 16 L of fresh broth and incubated further at 37 °C. Induction of ProP expression was initiated at an OD_{600} of 0.9 with 0.2% arabinose for 2 h. LacY expression was induced at an OD_{600} of 0.9 with 1 mM IPTG overnight at 26 °C. In both cases, cells were harvested and resuspended in 100 mL of lysis buffer (50 mM NaH_2PO_4, 300 mM NaCl, pH 8.0) and frozen at −80 °C.

The thawed harvested cells were incubated for 2 h in the presence of 100 μg/mL lysozyme, 30 μg/mL, DNase, 10 mM β-mercaptoethanol, and the following protease inhibitors; 0.5 mM phenylmethane-sulphonylfluoride, 2 mM tris(2-carboxyethyl)phosphine, 1 μg/mL leupeptin, 1 μg/mL aprotinin, 100 μg/mL soybean trypsin inhibitor, and 1 mM benzamidine. The cells were lysed with three passes through an Emulsiflex C-3 homogenizer (Avestin, Ottawa, ON, Canada) at 18,000 psi. After centrifugation (7000 ×*g* for 20 min) to remove unbroken cells, the supernatant was incubated for a further 2 h at 4 °C in the presence of the protease inhibitors. The membranes were then centrifuged at 135,000 ×*g* for 1 h at 4 °C and the membrane pellets resuspended, homogenized with a Wheaton 55 mL Teflon-glass hand homogenizer (Millville, NJ) in 50 mM NaH_2PO_4 and 300 mM NaCl.

2.3. Protein purification and reconstitution

Membrane fractions were solubilized at 4 °C for 1 h with 1% DDM in 50 mM NaH_2PO_4 with 300 mM NaCl, 0.5 mM phenylmethane-sulfonylfluoride, and 5 mM β-mercaptoethanol. After centrifugation at 100,000 ×*g* for 30 min to remove the unsolubilized material, the supernatant was incubated for 60 min at 4 °C with 10 mL TALON Superflow® metal-affinity resin. The resin was packed into a glass column and washed with 10 mM imidazole in a 50 mM NaH_2PO_4 buffer containing 300 mM NaCl and 0.075% DDM. The His-tagged protein was eluted with 200 mM imidazole and the pooled protein fraction concentrated to 1.1 mL in a Millipore Amicon 30,000 MW-cutoff concentrator (Burlington, MA) and applied to a 50 mL Superdex-200 resin column. The column was eluted with 50 mM NaH_2PO_4, 300 mM NaCl, 0.075% DDM, 10 mM β-mercaptoethanol, and 2 mM tris(2-carboxyethyl)phosphine.

The purified solubilized protein was reconstituted into membranes composed of either soybean asolectin or *E. coli* polar lipids by diluting 2.5 mg of the purified protein 20-fold with a similar solution containing either 30 mg of soybean asolectin or 15 mg of *E. coli* polar lipids solubilized with 1% cholate. Remaining detergent was then removed by dialysis (12–14 kDa cutoff) against 50 mM NaH_2PO_4 buffer containing 300 mM NaCl over 4 days with daily buffer changes. Pelleted proteoliposomes (2 h at 119,000 ×*g*) were resuspended in 5 mM Tris buffer at pH 7.5. Membrane incorporation was assessed using sucrose density gradients with steps of 2 mL each of 40% (w/v), 20% (w/v), 10% (w/v) and 3 mL of 0% (w/v) sucrose. In each case, 150 μg of reconstituted protein was deposited on the 0% (w/v) sucrose layer before the tubes were centrifuged for 20 h at 100,000 ×*g*. Fractions were assayed for both protein and lipid content.

2.4. FTIR spectroscopy

FTIR spectra were recorded on either an FTS 575 or an FTS 7000 spectrometer (Varian; Mississauga, ON) both equipped with a deuterated triglycine sulphate detector, as described elsewhere [19]. Except where noted, all protein samples were first exchanged into 2 mM ^2H_2O phosphate buffer, pH 7.4, by repeated centrifugation–resuspension cycles and stored under N_2 gas. After precisely 72 h at 4 °C, aliquots containing 250 μg of protein were deposited onto a CaF_2 window under a gentle stream of N_2 gas and then rehydrated with 8 μL of the same phosphate buffer. Samples sandwiched between two CaF_2 windows were placed in a thermostatically controlled transmission cell. For the secondary structure analysis, 4000-scan spectra were acquired at 2 cm^{-1} resolution. For the thermal denaturations, 128-scan spectra were recorded at 2 cm^{-1} resolution at 2 °C temperature increments over the range from 35 °C to 95 °C, with 20 min equilibration at each temperature.

All spectra were processed using Grams/AI v.7.01 (Galactic) and plotted using GraphPad Prism v4.03 (GraphPad Software, Inc.; La Jolla CA). Spectral deconvolution was performed between 1900 and 1500 cm^{-1} with $\gamma = 8.0$ and a Bessel smoothing of 80%, unless otherwise specified. In all cases, any traces of water vapour were removed from the spectra prior to deconvolution as described in Reid et al. [20].

3. Results

3.1. Purification and reconstitution of ProP into lipid membranes

Our first goal was to develop a protocol that would allow us to efficiently express, purify, and reconstitute ProP into proteoliposomes that are amenable to structural characterization using infrared spectroscopy. A new protocol was required because the commonly used reconstitution protocol for ProP typically yields proteoliposomes with lipid:protein ratios greater than 7000:1 on a mol:mol basis (calculated from [16]). While these high lipid–protein ratio proteoliposomes are ideal for transport assays (they have an internal diameter of 150 nm and only ~20 ProP molecules per vesicle), the resulting infrared spectra are dominated by intense lipid vibrations that overlap and thus distort the adjacent structurally sensitive protein amide I and II vibrations (Baenziger and Wood, unpublished observations). A reconstitution protocol yielding lower lipid–protein ratio proteoliposomes was thus required. Lower lipid–protein ratio vesicles are also optimal for recording infrared spectra using the attenuated total reflectance technique — a technique that can probe the subtle structural changes associated with protein conformational change [21,22]. With lower lipid–protein ratios, increasing amounts of protein are found within the volume sampled by the evanescent wave of the infrared light, thus increasing the magnitude of the absorption arising from the protein [23,24].

We purified ProP solubilized with the relatively mild detergent, DDM, using a two step protocol involving both a cobalt affinity and a gel-filtration column, and then assessed different reconstitution protocols for the generation of lower lipid–protein ratio proteoliposomes. We initially reconstituted the detergent-solubilized ProP into detergent-destabilized liposomes, as has been done previously [16], but using lower concentrations of lipids. We also reconstituted ProP by first mixing DDM-solubilized ProP with DDM-solubilized lipids, and then eliminating the detergent using Bio-Beads (BioRad Laboratories Ltd.; Hercules, CA) to form proteoliposomes. In our hands, these lower lipid:protein ratio reconstitution procedures met with less than optimal yields of reconstituted ProP (data not shown).

Finally, we adapted a protocol that was used previously by Patzlaff et al. to reconstitute functional LacY [25]. Affinity and gel-filtration purified DDM-solubilized ProP was slowly diluted 20-fold into a solution containing 1% cholate-solubilized lipid (either soybean asolectin or *E. coli* polar lipids) to bring the final DDM concentration below its critical micellar concentration, and the two detergents were then dialyzed away with several buffer changes. The dialysis protocol decreased the detergent to undetectable levels, as monitored by FTIR spectroscopy [26]. Sucrose density gradients showed that dialysis of the detergent led to the incorporation of ProP into the newly formed proteoliposomes (Fig. 1).

With five separate reconstitutions, this protocol led to consistent yields of incorporated ProP. SDS-PAGE shows that the protocol leads to a highly purified protein with calculated molecular weights in the 45–48 kDa range (Fig. 1), which is lower than the expected molecular weight of ProP-His_6 (54.8 kDa), but consistent with molecular weights calculated previously by SDS-PAGE for reconstituted ProP [16]. The lipid–protein ratios of the soybean asolectin proteoliposomes were estimated enzymatically (see Materials and methods) to be in the 150:1 to 300:1 mol:mol range, although the assay is specific for choline. As phosphatidylcholine represents only 14% to 24% of the total asolectin lipids, the measured lipid–protein ratios could correspond to lipid–protein ratios in the broad 625:1 to 2100:1 mol:mol range. Conversely, FTIR analysis of the lipid–protein ratios [26] showed that both the *E. coli* and asolectin lipid reconstitutions had comparable lipid-to-protein ratios typically in the 300–1000 mol:mol range. Although the resulting more densely-packed ProP proteoliposomes are likely not ideal for transport assays, infrared spectra of the lower lipid:protein ratio vesicles do not suffer from overlap of adjacent protein and lipid vibrations (see below). Significantly, the five separate purifications/reconstitutions each led to essentially identical infrared amide I band shapes indicative of a folded, highly α-helical conformation (see below).

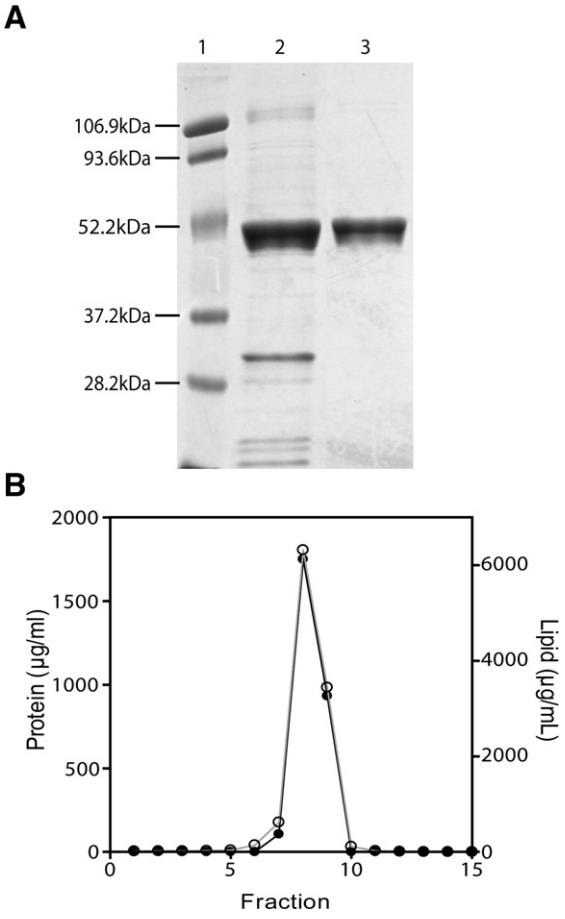

Fig. 1. (A) SDS-PAGE at different stages during purification of ProP. Lane 1: Molecular weight standard. Lane 2: ProP after elution from the cobalt-affinity column. Lane 3: ProP after elution from the Superdex gel filtration column. (B) Sucrose density gradient ultracentrifugation assay results for ProP reconstituted into asolectin lipids (the lipid enzymatic assay is specific for choline). Superposition of lipid (grey lines, open circles) and protein (black lines, filled circles) peaks suggests successful incorporation of ProP into the proteoliposome.

3.2. Characterization of secondary structure

We examined whether ProP contains the secondary structural features expected of a member of the major facilitator family of membrane transporters. FTIR spectra of the reconstituted ProP exhibit relatively intense vibrations characteristic of lipid, centered near 1730 cm^{-1} and 1450 cm^{-1}, and protein, between 1700 cm^{-1} and 1600 cm^{-1}, and centered near 1545 cm^{-1} (in ^1H_2O) or 1450 cm^{-1} (in ^2H_2O) (Fig. 2A). The secondary structure-sensitive amide I band located between 1600 and 1700 cm^{-1} is due primarily to the C=O stretching vibrations of the polypeptide backbone coupled to both C–N stretching and N–H bending modes [27]. This band is relatively sharp and symmetric with a maximum centered near 1656 cm^{-1} in spectra

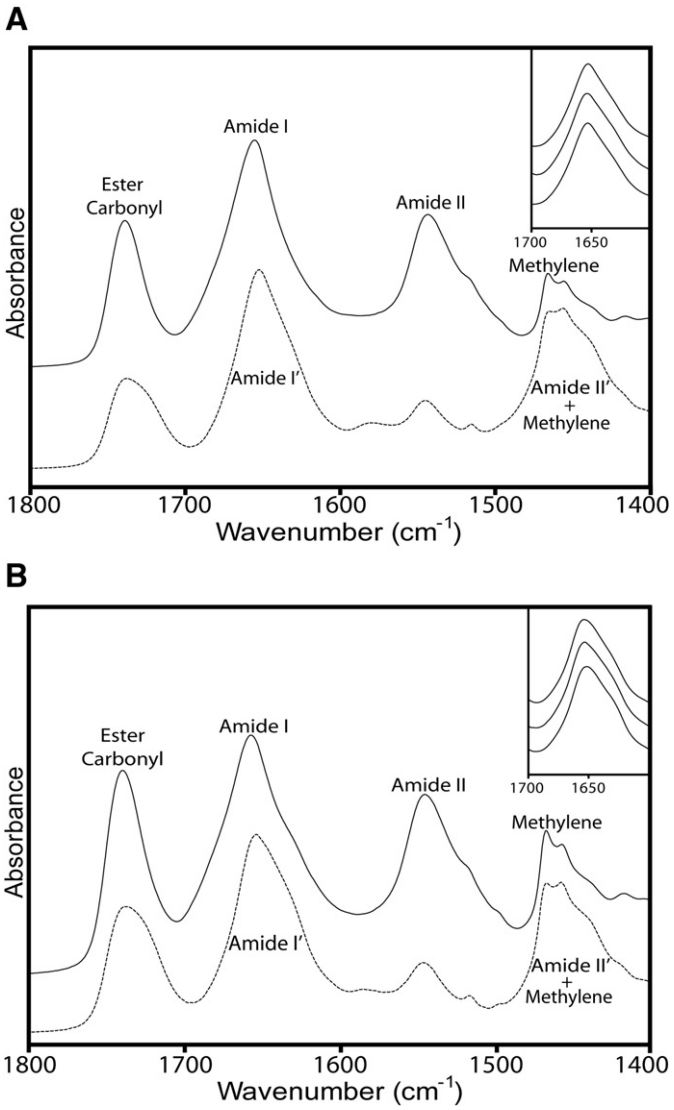

Fig. 2. FTIR spectra of reconstituted (A) ProP and (B) LacY, in ^1H_2O (solid lines) and after 72 h in ^2H_2O at 4 °C (dashed lines). Insets for ProP are reconstituted into soybean asolectin (top) and *E. coli* lipids (middle and bottom). The insets for LacY are all for reconstitutions into *E. coli* lipids. Typical amide I band intensities were in the 0.3 to 0.6 a.u. range.

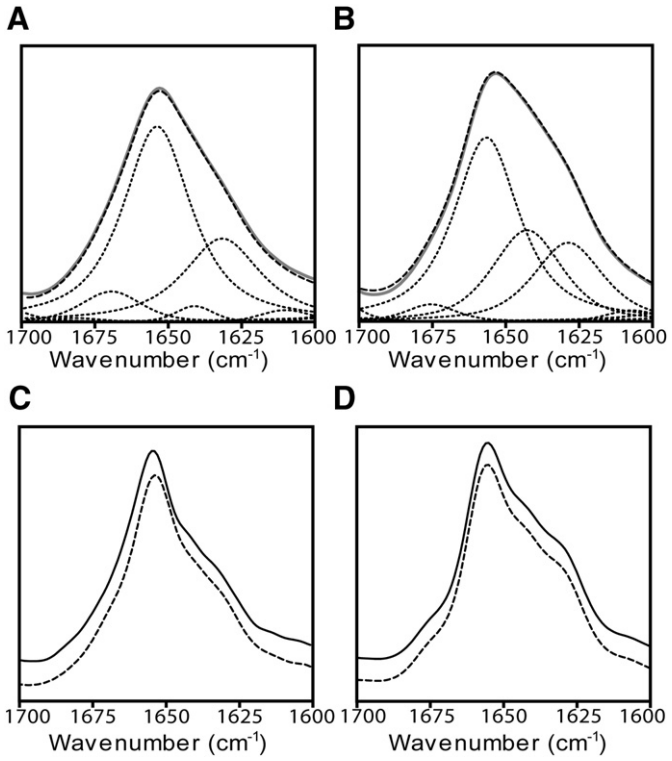

Fig. 3. Curve-fitting (A, B) of the amide I region in spectra recorded from ProP (A, C) and LacY (B, D). Experimental spectra (grey solid lines) are shown with curve-fit resultant (long-dashed lines) and putative component bands (short-dashed lines). Resolution enhancement (C, D) of the experimental (solid lines) and resultant curve-fit (dashed lines) spectra for ProP and LacY was performed to ascertain the accuracy of the curve fits. The spectra are offset to enhance the comparison. Deconvolution performed with $\gamma = 8.0$, smoothing = 70% (Bessel function) from 1800–1500 cm^{-1}.

dried from ^1H_2O. In ^2H_2O, the symmetric band undergoes a 4 cm^{-1} downshift in frequency to 1652 cm^{-1}, with relatively little change in band shape. The amide I shape and frequency maxima in both ^1H_2O and ^2H_2O are highly characteristic of a predominantly α-helical protein. The lack of substantive changes in band shape upon exposure to ^2H_2O suggests relatively little random coil or loop structures [28]. In fact, the amide I band shapes in ^1H_2O and ^2H_2O are very similar to the amide I band shapes that have been observed in spectra recorded under similar conditions from highly α-helical proteins, such as myoglobin and haemoglobin. In contrast, the ProP amide I band shapes differ substantially from those obtained from predominantly β-sheet or mixed α-helix/β-sheet proteins [27–29]. In our opinion, such comparisons of amide I band shapes provide the most accurate assessment of secondary structure content. These comparisons show that ProP is a predominantly α-helical transmembrane protein, consistent with its membership in the major facilitator superfamily of proteins. Our data are also consistent with the homology model of ProP presented by Wood et al. [9], which exhibits exclusively transmembrane α-helical secondary structures, interconnecting loops, and a C-terminal coiled extension. Note the reproducibility of the amide I band shapes from different affinity purification/reconstitutions into either soybean asolectin or *E. coli* lipids (inset of Fig. 2A).

Resolution enhancement reveals the underlying component bands that contribute to the overall amide I contour (Fig. 3A). Peaks identified from the deconvolved spectrum were used as input to curve fit the amide I band and thus estimate the secondary structure content of ProP, as shown in Fig. 3A. Although curve fit results are somewhat subject and depend on the choice of input parameters, the validity of the curve fit was assessed by comparing the resolution enhanced

Table 1
Comparison of the secondary structure estimates for ProP and LacY as determined by FTIR to those obtained from the homology model of ProP and the crystal structure of LacY

Band frequency (cm^{-1})[a]	Band assignment[b]	% secondary structure (curve fit)[c]		% secondary structure (other authors)[d]	
		ProP	LacY	ProP	LacY
1669–1676	β-turn/anti-parallel β-sheet	7	3	–	–
1653–1656	α-helix	61	51	69	77
1641–1646	Unordered	2	24	25	23
1629–1633	β-sheet[e]	29	21	6	–
1600–1700	Other	<1	<1	–	–

[a] Obtained from resolution-enhanced amide I band, see Fig. 3.
[b] Band assignments from Tamm and Tatulian [27].
[c] Obtained by curve fitting the amide I band. The accuracy of the curve-fit was assessed using the procedure of Méthot et al. [40].
[d] Calculated for ProP from the model of Wood et al. [9], and for LacY from the crystal structure of Guan et al. [3] (Protein Data Bank entry 2v8n).
[e] Note that α-helical proteins, such as myoglobin, exhibit weak bands in the region of infrared spectra that are characteristic of β-sheet (see text).

curve fit spectrum with the experimental resolution-enhanced data (Fig. 3C). Numerical estimates of the contributions of each secondary structure element to the two proteins are summarized in Table 1, suggesting further that ProP is a predominantly α-helical protein. Although deconvolution reveals the presence of weak underlying component bands that vibrate at frequencies typically attributed to β-sheet, even proteins such as myoglobin, with no β-sheet secondary structure, exhibit weak bands in these spectral regions [29,30,39]. The main amide I peak frequencies and thus overall amide I band shape unequivocally show that ProP is a predominantly α-helical protein. The interpretation of weak component bands in terms of the existence of specific secondary structural elements is, however, less reliable (see Discussion).

The infrared spectra of ProP do not contain any spectral features suggestive of the presence of denatured protein (spectra of denatured ProP are presented in Figs. 4A and 5A). Furthermore, the reconstituted ProP is thermally stable and shows no sign of denaturation until incubated at temperatures greater than 60 °C (see below and Fig. 5). The reconstituted ProP thus adopts a highly stable and predominantly α-helical fold, consistent with other members of the major-facilitator superfamily. The high thermal stability and high α-helical character both suggest that ProP adopts a native fold in our reconstituted membranes.

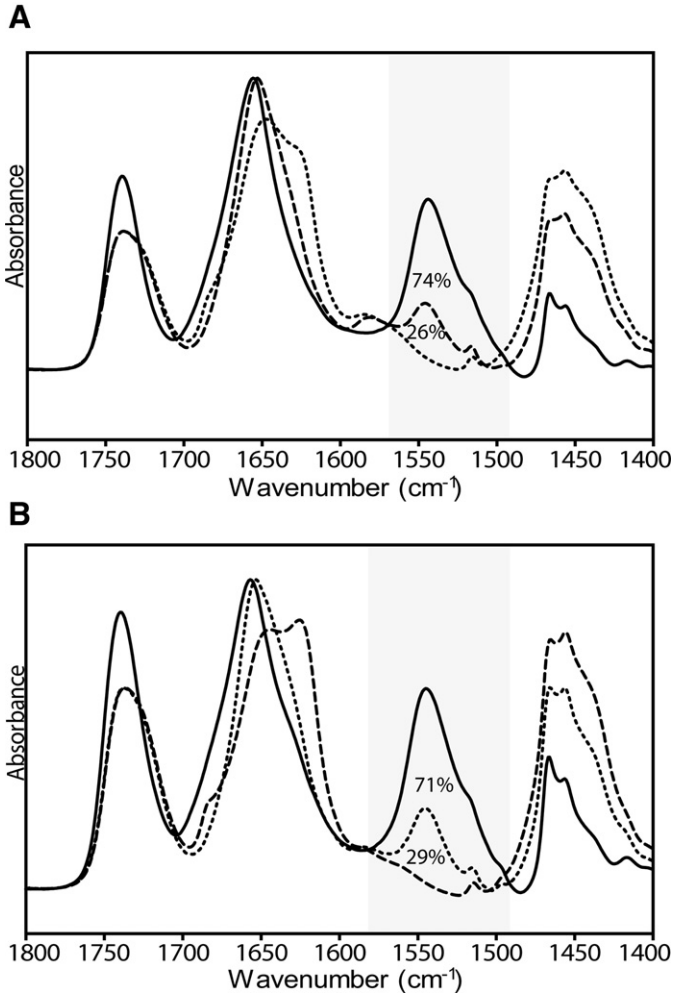

Fig. 4. Degree of hydrogen/deuterium exchange for (A) ProP and (B) LacY. Spectra of samples incubated in ^1H_2O buffer (solid lines), in ^2H_2O for 72 h at 4 °C (short-dashed lines), or boiled in ^2H_2O for 1 h (long-dashed lines). The labelled areas were calculated by integration under the amide II region, with the spectrum from the boiled sample as the baseline. See text. Note that the spectra recorded in ^1H_2O and after 3 days in ^2H_2O were scaled based on amide I band intensity. The spectra recorded in ^2H_2O were scaled to each other based on the lipid C=O stretching band intensities.

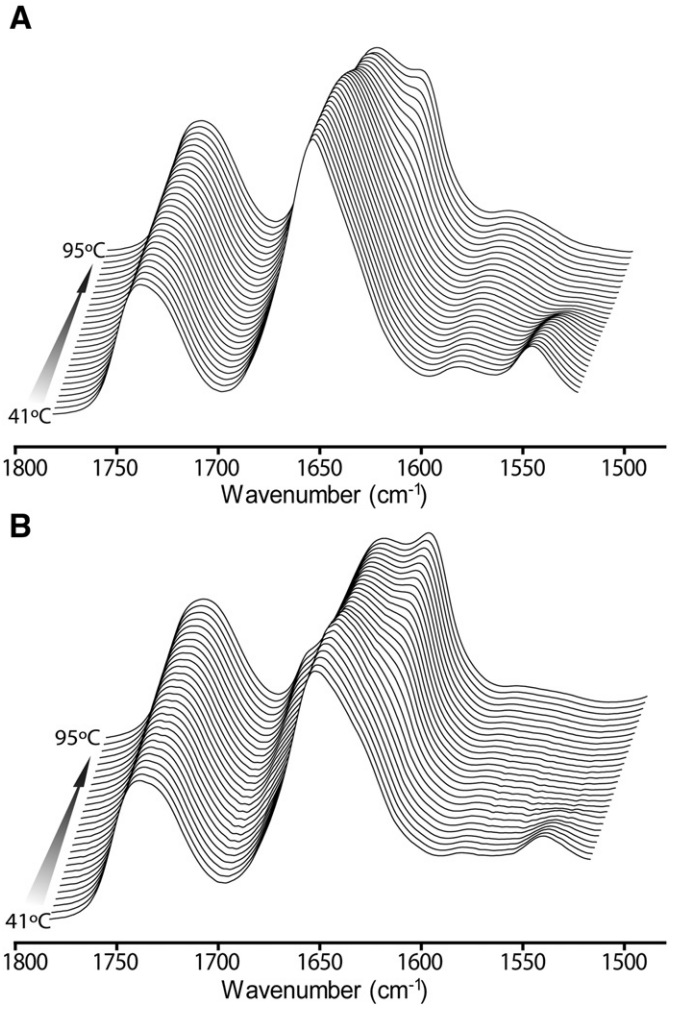

Fig. 5. Stacked plots of FTIR spectra at 2 °C intervals from the thermal denaturations of (A) ProP and (B) LacY. Spectra have been incrementally offset up and rightwards for display.

3.3. Structural comparison with LacY

To provide further insight into the structure of the reconstituted ProP and as a further test of the native fold, we compared the spectra obtained from ProP to those recorded under identical conditions from the identically purified and reconstituted homolog, LacY. The spectra of LacY presented in Fig. 2B are similar to those of ProP, in that the amide I bands are sharp and symmetric with a maximum in ^1H_2O near 1657 cm^{-1} that shifts down in frequency by only 4 cm^{-1} upon exposure to ^2H_2O. Deconvolution and secondary structure estimates for LacY reveal a similar content of α-helical secondary structures, as well as weak vibrations that occur in frequency regions typically attributed to β-sheet. Even the biophysical properties of the protein discussed below (i.e. the thermal stability and hydrogen–deuterium exchange characteristics) are remarkably similar. The comparison between ProP and LacY provides strong evidence that ProP adopts a structure consistent with other α-helical major facilitator superfamily members.

LacY is an α-helical major facilitator superfamily member whose crystal structure has been solved [2,3]. The structural interpretation of our infrared data recorded from reconstituted LacY is consistent with the solved structure of LacY. The infrared spectra recorded here for LacY are also very close (although of greater fidelity due to the lower lipid–protein ratios and higher signal-to-noise ratios) to those that have been recorded previously from membrane reconstituted and functional LacY [33]. The close correlation between the structural data

obtained here and the data obtained elsewhere for LacY serves as a control to show that our reconstitution protocol leads to proteoliposomes containing LacY, which adopts a native fold. The close correlation between the infrared data obtained for ProP and LacY (see above and below) strongly suggests that the structural and biophysical data obtained here for ProP also corresponds to a native fold of ProP in our reconstituted membranes.

3.4. Extent of solvent exchange upon exposure to ^2H_2O

We next measured the extent to which the peptide hydrogens in ProP and LacY exchange for deuterium after exposure to ^2H_2O. The extent of peptide hydrogen/deuterium exchange was of interest because the transmembrane segments in many α-helical membrane proteins are shielded from aqueous solution and thus resistant to exchange. The percentage of transmembrane peptide hydrogens that remain protiated after prolonged exposure to ^2H_2O often correlates with the percentage of peptides that reside within the lipid bilayer [30–32]. In contrast, most of the transmembrane peptide hydrogens in LacY readily exchange with protons/deuterium atoms in the solvent [33], possibly due to the high solvent accessibility of the transmembrane domain. The high aqueous solvent exposure is thought to underlie transport of solutes across the membrane [34]. Given that ProP is a member of the same major facilitator super-family of proteins and is thought to exhibit a similar transport mechanism [35], it was of interest to ascertain whether the transmembrane peptide hydrogens in ProP undergo relatively extensive hydrogen/deuterium exchange.

We examined the extent of peptide hydrogen–deuterium exchange after 72 h exposure to ^2H_2O at 4 °C by measuring the residual area of the amide II vibration (primarily peptide N–^{1}H bending coupled to C–N stretching) centered near 1545 cm^{-1}. Upon peptide hydrogen/deuterium exchange, the amide II vibration shifts down in frequency to near 1450 cm^{-1}. The residual amide II band area is thus proportional to the number of peptides that remain in the protiated state. Comparison of the residual amide II band area of ProP after 72 h exposure to ^2H_2O at 4 °C to the residual amide II band areas in spectra recorded in ^1H_2O (100% peptide N–^{1}H) and in ^2H_2O after boiling for 1 h (0% peptide N–^{2}H) shows that roughly 70% of the peptide hydrogens in ProP undergo exchange after the 72 hour time period. Given that roughly 30% of the peptide hydrogens in ProP [9] are thought to exist outside of transmembrane segments, it can be concluded that the transmembrane α-helices of ProP do undergo relatively extensive peptide hydrogen/deuterium exchange, consistent with previous findings for LacY.

We estimate, however, that 26% ± 1% ($n = 3$) of ProP peptide hydrogens are resistant to hydrogen/deuterium exchange after 72 h in ^2H_2O at 4 °C. We find that under identical conditions, roughly 29% ± 2% ($n = 3$) of LacY peptide hydrogens are also resistant to exchange (Fig. 4B). Although the transmembrane domains of both ProP and LacY undergo more extensive hydrogen/deuterium exchange than the transmembrane domains of other transmembrane α-helical proteins, there is a proportion of exchange-resistant transmembrane α-helical peptide hydrogens in both proteins. The subtle differences between our findings and previously published data likely reflect a combination of experimental and technical factors (see Discussion).

3.5. Thermal stability

Given the high levels of transmembrane peptide/hydrogen exchange, we were interested in determining the thermal stability of ProP in the reconstituted membranes. FTIR spectra recorded as a function of temperature (Fig. 5) show that both ProP and LacY undergo a temperature-dependent loss of intensity between 1650 and 1655 cm^{-1}, with a concomitant increase in intensity at roughly 1680 cm^{-1} and 1624 cm^{-1} (see Fig. 6). In both cases, these spectral changes have been attributed to denaturation and subsequent formation of intermolecular

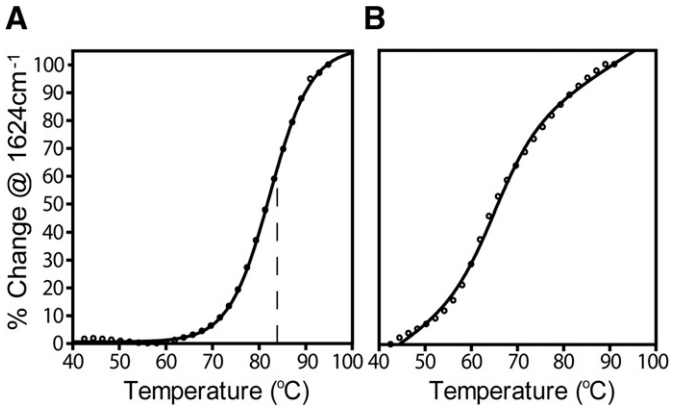

Fig. 6. Relative intensity changes versus temperature plots for the denaturation experiments depicted in Fig. 5 for (A) ProP and (B) LacY. The intensities were plotted at 1624 cm^{-1} from spectra deconvolved with $\gamma = 8.0$, smoothing = 80% (Bessel function) from 1900–1300 cm^{-1}. The plotted intensity versus temperature plots have been fit with a curve composed of a linear and a Boltzmann sigmoidal function. The T_d for ProP given by the midpoint of the rapid phase of the Boltzmann function, marked here by a dashed vertical line. See text.

hydrogen bonds [36,37]. Spectral changes suggestive of denaturation begin to appear at temperatures close to 60 °C and continue beyond the temperature capabilities of our FTIR sample accessory.

With ProP, the spectral changes were fit with a Boltzmann sigmoidal curve yielding a thermal denaturation temperature (50% denaturation) of 84 ± 1.3 °C ($n = 3$). The denaturation curves for LacY are reproducibly more complex (Fig. 6B) and do not follow a typical sigmoidal pattern, suggesting that denaturation is not a simple two-step reaction between fully folded and fully unfolded states. Regardless, the spectral changes indicative of denaturation for LacY begin at a temperature roughly 10 °C below the onset temperature for denaturation of ProP. ProP has also not advanced to the same denatured state as LacY at the highest studied temperatures (95 °C). Although we cannot assess whether ProP exhibits similar complex denaturation characteristics (due to the greater thermal stability of ProP), it is clear that ProP is more thermally stable than LacY.

It is intriguing to note that increasing temperature leads to loss of amide II band intensity and thus exchange of the exchange-resistant peptide hydrogens in both ProP and LacY, but complete exchange occurs in temperatures below those at which signs of denaturation appear. In contrast, we have found with other membrane proteins that complete peptide hydrogen/deuterium exchange typically occurs upon thermal denaturation [19,38]. As noted, the relatively extensive exchange of peptide hydrogens in both ProP and LacY is likely due to the high solvent accessibility of these solute transport proteins. It seems plausible that the enhanced exchange in both proteins with increasing temperature may result from a temperature-dependent increase in the rate of interconversion between conformational states, and thus an even greater exposure of transmembrane peptide hydrogens to aqueous solvent.

4. Discussion

Much of the current work focused on elucidating the mechanisms of ProP function assumes, based on sequence homology, that ProP exhibits structural homology to other members of the major facilitator super-family of integral membrane proteins, but there is little direct structural data supporting this contention. The biophysical data presented here offers the first direct physical insight into ProP structure and provides compelling evidence that ProP adopts a structure consistent with other members of the major facilitator super-family members. Our data are also consistent with ProP adopting a transmembrane α-helical structure similar to that proposed in the homology model of Wood et al. [9]. These conclusions are based on the following observations.

First, our spectral analysis shows unequivocally that ProP is a highly α-helical membrane protein. The amide I band shapes in $^{1}H_2O$ and $^{2}H_2O$ are both sharp and symmetric with frequency maxima between 1650 and 1655 cm^{-1}, all of which are characteristic of predominantly α-helical proteins. Although our secondary structural predictions suggest an α-helical content for ProP that is slightly lower than expected, this may be because ProP exhibits weak amide I vibrations that occur in regions typically attributed to β-sheet. One possible explanation is that some of the transmembrane helices in ProP are distorted from the canonical α-helical structure (i.e. 3.6 residues per turn) leading to vibrations that occur in non α-helical regions of the infrared spectrum. Distorted transmembrane helical structures were proposed in the homology model of Wood et al. [9]. Significantly, the amide I band shapes of ProP are similar to those obtained for the major facilitator super-family member, LacY. Furthermore the spectra of both ProP and LacY are similar to those that have been obtained for other highly α-helical proteins including myoglobin and haemoglobin. The latter also exhibit weak vibrations in these same "β-sheet" spectral regions [29,30,39]. Our spectral data thus provide conclusive biophysical evidence that ProP adopts a predominantly transmembrane α-helical fold, consistent with other members of the major facilitator superfamily of proteins.

Second, we find that 70–75% of the peptide hydrogens in ProP exchange for deuterium after 72 h exposure to $^{2}H_2O$ at 4 °C. Given that the majority of the peptide hydrogens in ProP (~70%) are thought to be located within the transmembrane helical segments, our finding shows that the transmembrane peptides in ProP are unusually exposed to aqueous solvent. In contrast, we have found that the number of peptide hydrogens that remain unexchanged for deuterium after prolonged exposure (72 h at 4 °C) in the nicotinic acetylcholine receptor correlates with the number of peptide hydrogens found within the membrane [30]. The transmembrane α-helices of many other proteins are also highly resistant to peptide hydrogen/deuterium exchange. In contrast, a high solvent accessibility of the transmembrane peptides has been reported for LacY [25,33,34]. The fact that the transmembrane domains of both ProP and LacY share similar exchange characteristics suggests that the transmembrane domains of both proteins are equally accessible to solvent and thus both adopt transmembrane structures consistent with the alternating-access model of solute transport.

We do find that 25–30% of the ProP peptide hydrogens are resistant to exchange for deuterium after 72 h in $^{2}H_2O$ at 4 °C. The number of exchange resistant peptide hydrogens measured here for ProP is slightly higher than reported previously for LacY, where it was suggested that only 5% of the peptide hydrogens remain unexchanged for deuterium after 24 h at 20 °C in $^{2}H_2O$ [33]. The 25–30% exchange resistant peptide hydrogens reported here for ProP, however, are similar to the number of exchange resistant peptide hydrogens that we measure for LacY under identical experimental conditions. The minor differences between the levels of exchange resistant peptide hydrogens estimated in this versus other studies are likely due to several factors. Our exchange experiments were performed at 4 °C, as opposed to 20 °C. Given that the rates of ProP and LacY peptide hydrogen–deuterium exchange increase with increasing temperature (Fig. 5), the lower temperature of our exchange experiments could account for the reduced levels of peptide hydrogen–deuterium exchange in our samples. The higher lipid:protein ratio of the reconstituted LacY samples used by le Coutre et al. [33] leads to spectral overlap between lipid and protein vibrations, making an accurate assessment of the intensity corresponding to unexchanged peptide hydrogens near 1540 cm^{-1} more difficult. Finally, to facilitate an accurate measurement of the number of exchange resistant peptide hydrogens, we measured the amide II intensities near 1540 cm^{-1} corresponding to both 0% (100% N–^{1}H) and 100% (100% N–^{2}H) exchange in spectra of both ProP and LacY. These extremes must be calculated to accurately relate residual amide II band intensities to the percentage of peptide hydrogens that remain after a given time of exposure to $^{2}H_2O$. The slightly different exchange conditions coupled with the noted technical differences between the studies can easily account for the minor variations in the reported percentages of exchange-resistant peptide hydrogens.

Third, we show here for both ProP and LacY that the exchange-resistant transmembrane peptide hydrogens can be exchanged completely with deuterium with increasing temperature. Surprisingly, this enhanced hydrogen/deuterium exchange in both proteins occurs at temperatures below those that lead to denaturation. This contrasts findings from other proteins where the exchange of typically exchange-resistant transmembrane peptide hydrogens only occurs at temperatures that coincide with protein denaturation [19,38]. The similar temperature-dependencies of peptide hydrogen/deuterium exchange for the two proteins provide additional support for structural similarity between LacY and ProP in their transmembrane regions.

We do, however, detect subtle differences in some of the structural properties of the two proteins. The amide I band shapes for ProP exhibit a slightly more α-helical character than LacY, which could be due to the putative C-terminal coiled coil extension. ProP is more thermally stable than LacY. Higher temperatures are also required to stimulate the exchange of the peptide hydrogens in ProP. It is interesting to speculate that a more thermally stable conformer of ProP could result from homo-dimerization of the protein in the bilayer, mediated by the C-terminal coiled-coil structure. The increased stability of ProP may enhance its ability to respond to osmotic stress when the bacterium is exposed to harsh environments.

Our data show conclusively that the transmembrane protein, ProP, adopts a predominantly α-helical secondary structure with solvent accessible transmembrane α-helices. Exchange of the peptide hydrogens in ProP is greatly enhanced by increasing temperature, despite the fact that ProP exhibits relatively high thermal stability. The structure and solvent exchange characteristics are very similar to those of the homolog LacY. We thus conclude that ProP adopts a transmembrane α-helical structure with a highly accessible aqueous binding site. Our results provide the first physical evidence that ProP adopts a structure consistent with other members of the major facilitator superfamily of membrane transporters. Further structural studies using the protocol developed here should provide more detailed insight into the structural features that are associated with ProP conformational change and that underlie the lipid sensitivity of this important osmoprotectant transporter.

Acknowledgements

We thank Shuzhi Wang and Ngoc Vuong for their technical assistance, and Drs. Wood and Kaback for supplying cells/plasmids for the expression of ProP and LacY, respectively.

References

[1] M.H. Saier Jr., J.T. Beatty, A. Goffeau, K.T. Harley, W.H. Heijne, S.C. Huang, D.L. Jack, P.S. Jähn, K. Lew, J. Liu, S.S. Pao, I.T. Paulsen, T.T. Tseng, P.S. Virk, The major facilitator superfamily, J. Mol. Microbiol. Biotechnol. 1 (1999) 257–279.
[2] J. Abramson, I. Smirnova, V. Kasho, G. Verner, H.R. Kaback, S. Iwata, Structure and mechanism of the lactose permease of *Escherichia coli*, Science 301 (2003) 610–615.
[3] L. Guan, O. Mirza, G. Verner, S. Iwata, H.R. Kaback, Structural determination of wild-type lactose permease, Proc. Natl. Acad. Sci. U. S. A. 104 (2007) 15294–15298.
[4] J.A. Heymann, R. Sarker, T. Hirai, D. Shi, J.L. Milne, P.C. Maloney, S. Subramaniam, Projection structure and molecular architecture of OxlT, a bacterial membrane transporter, EMBO J. 20 (2001) 4408–4413.
[5] Y. Huang, M.J. Lemieux, J. Song, M. Auer, D.N. Wang, Structure and mechanism of the glycerol-3-phosphate transporter from *Escherichia coli*, Science 301 (2003) 616–620.
[6] J. Abramson, H.R. Kaback, S. Iwata, Structural comparison of lactose permease and the glycerol-3-phosphate antiporter: members of the major facilitator superfamily, Curr. Opin. Struct. Biol. 14 (2004) 413–419.

[7] J.L. Milner, S. Grothe, J.M. Wood, Proline porter II is activated by a hyperosmotic shift in both whole cells and membrane vesicles of *Escherichia coli* K12, J. Biol. Chem. 263 (1988) 14900–14905.
[8] B. Poolman, J.J. Spitzer, J.M. Wood, Bacterial osmosensing: roles of membrane structure and electrostatics in lipid–protein and protein–protein interactions, Biochim. Biophys. Acta 1666 (2004) 88–104.
[9] J.M. Wood, D.E. Culham, A. Hillar, Y.I. Vernikovska, F. Liu, J.M. Boggs, R.A. Keates, A structural model for the osmosensor, transporter, and osmoregulator ProP of *Escherichia coli*, Biochemistry 44 (2005) 5634–5646.
[10] F. Liu, D.E. Culham, Y.I. Vernikovska, R.A. Keates, J.M. Boggs, J.M. Wood, Structure and function of transmembrane segment XII in osmosensor and osmoprotectant transporter ProP of *Escherichia coli*, Biochemistry 46 (2007) 5647–5655.
[11] A. Hillar, D.E. Culham, Y.I. Vernikovska, J.M. Wood, J.M. Boggs, Formation of an antiparallel, intermolecular coiled coil is associated with in vivo dimerization of osmosensor and osmoprotectant transporter ProP in *Escherichia coli*, Biochemistry 44 (2005) 10170–10180.
[12] D.E. Culham, B. Tripet, K.I. Racher, R.T. Voegele, R.S. Hodges, J.M. Wood, The role of the carboxyl terminal alpha-helical coiled-coil domain in osmosensing by transporter ProP of *Escherichia coli*, J. Mol. Recognit. 13 (2000) 309–322.
[13] Y. Tsatskis, J. Khambati, M. Dobson, M. Bogdanov, W. Dowhan, J.M. Wood, The osmotic activation of transporter ProP is tuned by both its C-terminal coiled-coil and osmotically induced changes in phospholipids composition, J. Biol. Chem. 280 (2005) 41387–41394.
[14] Y. Tsatskis, S.C. Kwok, E. Becker, C. Gill, M.N. Smith, R.A. Keates, R.S. Hodges, J.M. Wood, Core residue replacements cause coiled-coil orientation switching in vitro and in vivo: structure–function correlations for osmosensory transporter ProP, Biochemistry 47 (2008) 60–72.
[15] K.I. Racher, D.E. Culham, J.M. Wood, Requirements for osmosensing and osmotic activation of transporter ProP from *Escherichia coli*, Biochemistry 40 (2001) 7324–7333.
[16] K.I. Racher, R.T. Voegele, E.V. Marshall, D.E. Culham, J.M. Wood, H. Jung, M. Bacon, M.T. Cairns, S.M. Ferguson, W.J. Liang, P.J. Henderson, G. White, F.R. Hallett, Purification and reconstitution of an osmosensor: transporter ProP of *Escherichia coli* senses and responds to osmotic shifts, Biochemistry 38 (1999) 1676–1684.
[17] L. Guan, I.N. Smirnova, G. Verner, S. Nagamori, H.R. Kaback, Manipulating phospholipids for crystallization of a membrane transport protein, Proc. Natl. Acad. Sci. U. S. A. 103 (2006) 1723–1726.
[18] B. Miroux, J.E. Walker, Over-production of proteins in *Escherichia coli*: mutant hosts that allow synthesis of some membrane proteins and globular proteins at high levels, J. Mol. Biol. 260 (1996) 289–298.
[19] C.L. Carswell, M.D. Rigden, J.E. Baenziger, Expression, purification, and structural characterization of CfrA, a putative iron transporter from *Campylobacter jejuni*, J. Bacteriol. 190 (2008) 5650–5662.
[20] S.E. Reid, D.J. Moffatt, J.E. Baenziger, The selective enhancement and subsequent subtraction of atmospheric water vapour contributions from Fourier transform infrared spectra of proteins, Spectrochim. Acta, Part A: Mol. Biomol. Spectrosc. 52 (1996) 1347–1356.
[21] S.E. Ryan, D.G. Hill, J.E. Baenziger, Dissecting the chemistry of nicotinic receptor-ligand interactions with infrared difference spectroscopy, J. Biol. Chem. 277 (2002) 10420–10426.
[22] J.E. Baenziger, S.E. Ryan, M.M. Goodreid, N.Q. Vuong, R.M. Sturgeon, C.J.B. daCosta, Lipid composition alters drug action at the nicotinic acetylcholine receptor, Mol. Pharmacol. 73 (2008) 880–890.
[23] J.E. Baenziger, S.E. Ryan, V.C. Kane-Dickson, Membrane receptor-ligand interactions probed by attenuated total reflectance infrared differences spectroscopy, in: Vasilis G. Gregoriou, Mark S. Braiman (Eds.), Vibrational Spectroscopy of Biological and Polymeric Materials, Taylor and Francis Group, 2006, pp. 325–351.
[24] J.E. Baenziger, C.J.B. daCosta, Membrane protein structure and conformational change probed using Fourier transform infrared spectroscopy, in: Eva Pebay-Peyroula (Ed.), Biophysical Analysis of Membrane Proteins, Wiley-VCH, 2008, pp. 259–288.
[25] J.S. Patzlaff, J.A. Moeller, B.A. Barry, R.J. Brooker, Fourier transform infrared analysis of purified lactose permease: a monodisperse lactose permease preparation is stably folded, alpha-helical, and highly accessible to deuterium exchange, Biochemistry 37 (1998) 15363–15375.
[26] C.J.B. daCosta, J.E. Baenziger, A rapid method for assessing lipid:protein and detergent:protein ratios in membrane-protein crystallization, Acta Crystallogr. D Biol. Crystallogr. 59 (2003) 77–83.
[27] L.K. Tamm, S.A. Tatulian, Infrared spectroscopy of proteins and peptides in lipid bilayers, Q. Rev. Biophys. 30 (1997) 365–429.
[28] J.E. Baenziger, J.P. Chew, Desensitization of the nicotinic acetylcholine receptor mainly involves a structural change in solvent-accessible regions of the polypeptide backbone, Biochemistry 36 (1997) 3617–3624.
[29] D.M. Byler, H. Susi, Examination of the secondary structure of proteins by deconvolved FTIR spectra, Biopolymers 25 (1986) 469–487.
[30] N. Méthot, J.E. Baenziger, Secondary structure of the exchange-resistant core from the nicotinic acetylcholine receptor probed directly by infrared spectroscopy and hydrogen/deuterium exchange, Biochemistry 37 (1998) 4815–14822.
[31] T.N. Earnest, J. Herzfeld, K.J. Rothschild, Polarized Fourier transform infrared spectroscopy of bacteriorhodopsin. Transmembrane alpha helices are resistant to hydrogen/deuterium exchange, Biophys. J. 58 (1990) 1539–1546.
[32] J.E. Baenziger, N. Méthot, Fourier transform infrared and hydrogen/deuterium exchange reveal an exchange-resistant core of alpha-helical peptide hydrogens in the nicotinic acetylcholine receptor, J. Biol. Chem. 270 (1995) 29129–29137.
[33] J. le Coutre, L.R. Narasimhan, C.K. Patel, H.R. Kaback, The lipid bilayer determines helical tilt angle and function in lactose permease of *Escherichia coli*, Proc. Natl. Acad. Sci. U. S. A. 94 (1997) 10167–10171.
[34] L. Guan, H.R. Kaback, Lessons from lactose permease, Annu. Rev. Biophys. Biomol. Struct. 35 (2006) 67–91.
[35] D.E. Culham, T. Romantsov, J.M. Wood, Roles of K^+, H^+, H_2O, and $\Delta\Psi$ in solute transport mediated by major facilitator superfamily members ProP and LacY, Biochemistry 47 (2008) 8176–8185.
[36] J.L. Arrondo, H.H. Mantsch, N. Mullner, S. Pikula, A. Martonosi, Infrared spectroscopic characterization of the structural changes connected with the E1–E2 transition in the Ca^{2+}-ATPase of sarcoplasmic reticulum, J. Biol. Chem. 262 (1987) 9037–9043.
[37] W.Z. He, W.R. Newell, P.I. Haris, D. Chapman, J. Barber, Protein secondary structure of the isolated photosystem II reaction center and conformational changes studies by Fourier transform infrared spectroscopy, Biochemistry 30 (1991) 4552–4559.
[38] C.J.B. daCosta, D.E. Kaiser, J.E. Baenziger, Role of glycosylation and membrane environment in nicotinic acetylcholine receptor stability, Biophys. J. 88 (2005) 1755–1764.
[39] N. Méthot, B.D. Ritchie, M.P. Blanton, J.E. Baenziger, Structure of the pore-forming transmembrane domain of a ligand-gated ion channel, J. Biol. Chem. 276 (2001) 23726–23732.
[40] N. Méthot, M.P. McCarthy, J.E. Baenziger, Secondary structure of the nicotinic acetylcholine receptor: implications for structural models of a ligand-gated ion channel, Biochemistry 33 (1994) 7709–7717.